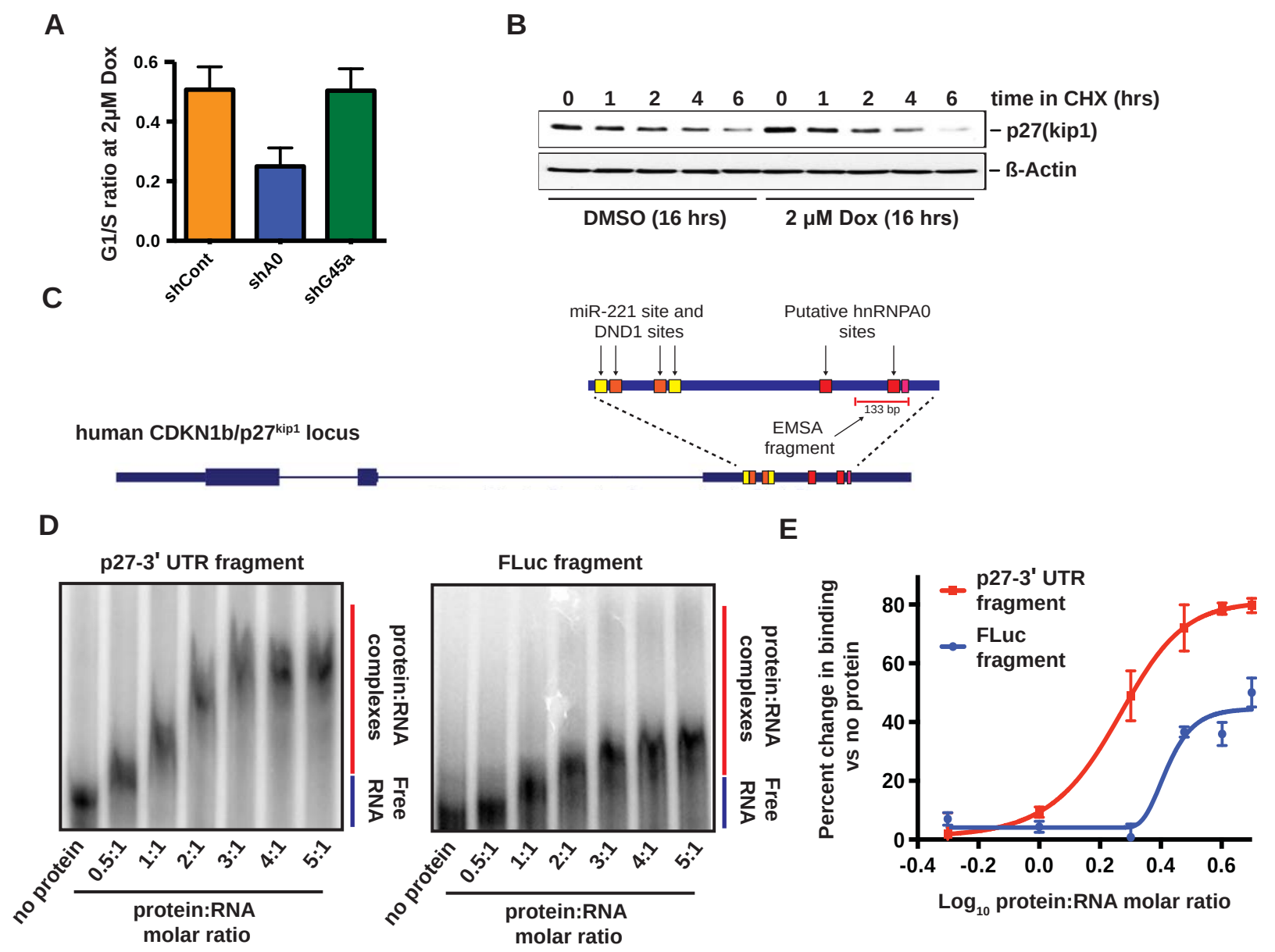
A
G1/S ratio at 2μM Dox
0.6
0.4
0.2
0.0
shCont
shA0
shG45a
B
0 1 2 4 6 0 1 2 4 6 time in CHX (hrs)
– p27(kip1)
– ß-Actin
DMSO (16 hrs)
2 μM Dox (16 hrs)
C
miR-221 site and DND1 sites
Putative hnRNPA0 sites
133 bp
EMSA fragment
human CDKN1b/p27kip1 locus
D
p27-3' UTR fragment
FLuc fragment
protein:RNA complexes
Free RNA
no protein
0.5:1
1:1
2:1
3:1
4:1
5:1
protein:RNA molar ratio
E
p27-3' UTR fragment
FLuc fragment
Percent change in binding vs no protein
80
60
40
20
0
-0.4
-0.2
0.0
0.2
0.4
0.6
Log10 protein:RNA molar ratio

Figure S1. A focused screen implicates p27(Kip1) as an hnRNPA0-dependent G1/S regulator. Related to Figure 1. (A) Quantification of flow cytometry profiles from Figure 1A expressed as G1+S/G2 ratio. Bars represent mean +/- SEM n=2. **(B)** Western blot analysis of p27 protein levels after doxorubicin treatment and subsequent cycloheximide treatment time course to determine p27 protein stability changes in response to DNA damage. Raw data that are expressed graphically in Figure 1F. **(C)** UCSC genome browser representation of the cdkn1b/p27^{kip1} locus. Schematic depicts the cdkn1b gene architecture. Zoomed in section of the 3′ UTR illustrates two putative perfect hnRNPA0 binding sites and where they are in relation to other post-transcriptional regulators of p27^{kip1}. Red line depicts the section of the 3′ UTR used for *in vitro* binding analysis that contains a perfect hnRNPA0 binding site AAUUUA red box (Wang et al., 2013) and a very good hnRNPA0 binding site AUUUA pink box. **(D)** Representative electromobility shifts assays (EMSAs) with recombinant hnRNPA0 RRM domains and a fragment of the p27^{kip1} 3′ UTR or Firefly luciferase as a negative control. **(E)** Quantification of multiple EMSA experiments expressed as percent bound probe relative to a reaction where no protein was added individual points represent the mean +/- SEM n = 3-5.

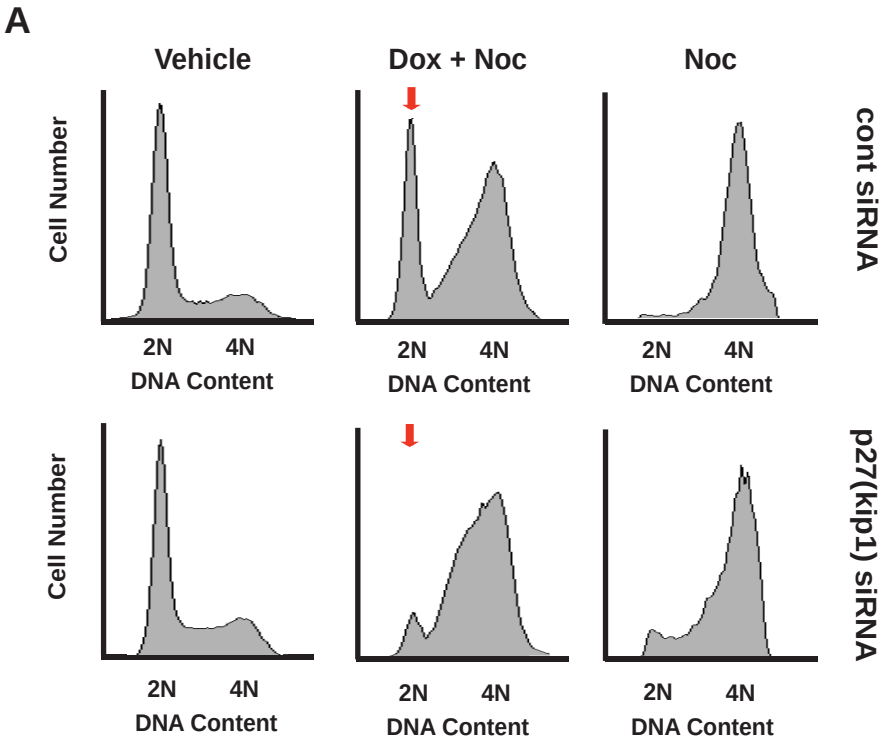
A
Vehicle
Dox + Noc
Noc
Cell Number
cont siRNA
p27(kip1) siRNA
2N
4N
DNA Content

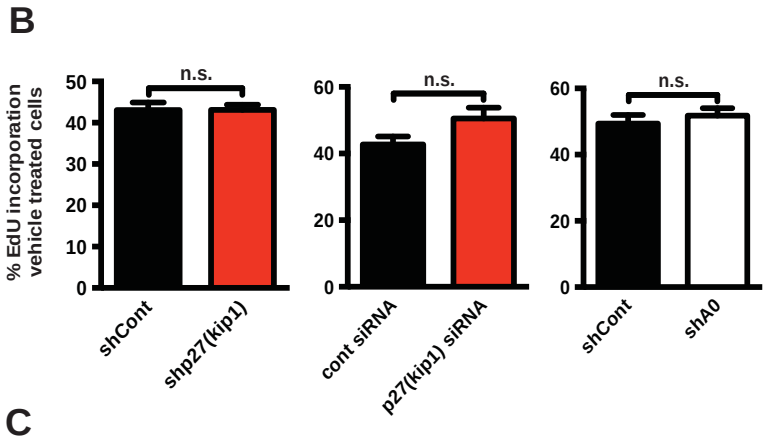
B
% EdU incorporation vehicle treated cells
n.s.
shCont
shp27(kip1)
cont siRNA
p27(kip1) siRNA
shCont
shA0

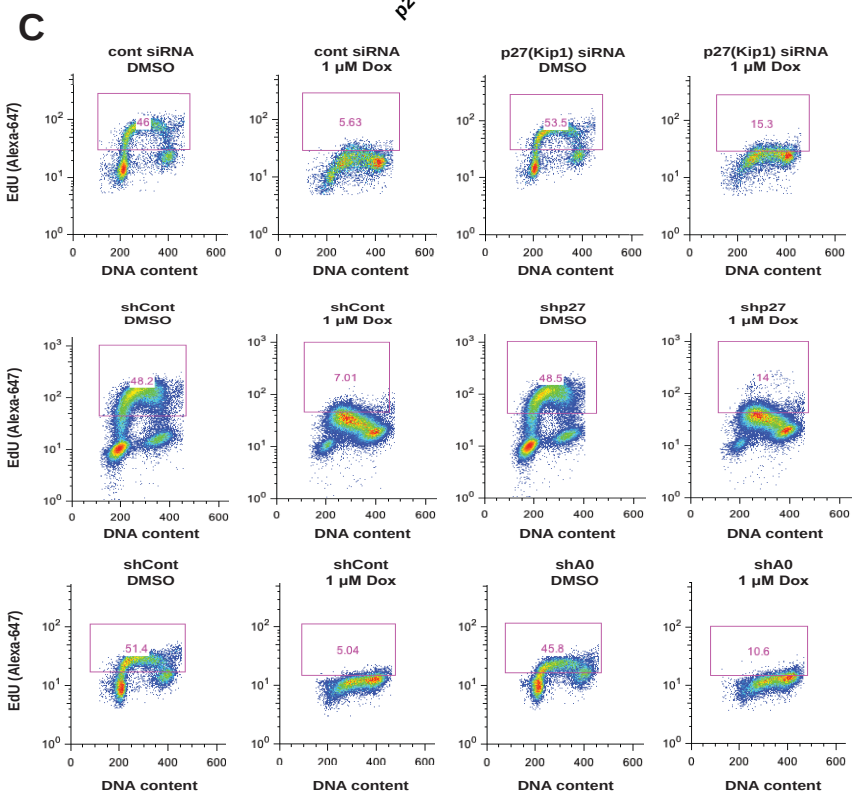
C
cont siRNA DMSO
cont siRNA 1 μM Dox
p27(Kip1) siRNA DMSO
p27(Kip1) siRNA 1 μM Dox
shCont DMSO
shCont 1 μM Dox
shp27 DMSO
shp27 1 μM Dox
shCont DMSO
shCont 1 μM Dox
shA0 DMSO
shA0 1 μM Dox
EdU (Alexa-647)
DNA content

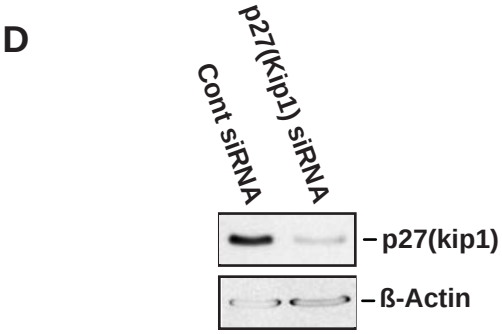
D
Cont siRNA
p27(Kip1) siRNA
p27(kip1)
ß-Actin

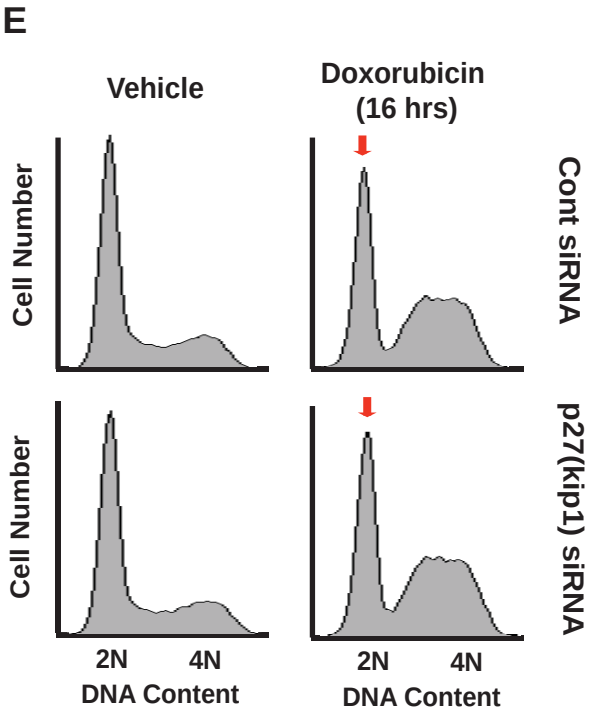
E
Vehicle
Doxorubicin (16 hrs)
Cont siRNA
p27(kip1) siRNA
Cell Number
2N
4N
DNA Content

Figure S2. p27(Kip1) controls the DNA damage-induced G1/S checkpoint in *p53*-deficient cells. Related to Figure 2. (A) Cell cycle analysis following nocodazole-trap in H1299 cells depleted on p27(Kip1) by siRNA. Briefly cells were treated with 1 μM doxorubicin for 4 hrs followed by the addition of 250 ng/mL of nocodazole for a further 24 hrs. Cell cycle was analyzed by propidium iodide staining. Red arrow signifies the G1 population. **(B)** p27 depletion does not effect EdU incorporation in the absence of DNA damage. EdU incorporation assays related to Figure 2D-E. **(C)** Representative cell cycle/EdU flow cytometry plots used for quantification in Figure 2E and S2B **(D)** and **(E)** p27 knockdown does not effect G1 arrest in *p53*-proficient A549 cells. **(D)** Efficient depletion of p27 by siRNA in A549 cells. **(E)** Cell cycle analysis of A549 cells treated with doxorubicin for 16 hrs demonstrates no difference in G1 arrest upon p27 knockdown.

A

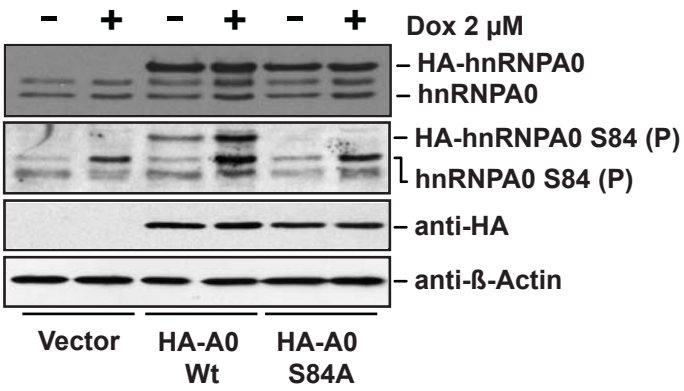
- + - + - +
Dox 2 µM
– HA-hnRNPA0
– hnRNPA0
– HA-hnRNPA0 S84 (P)
hnRNPA0 S84 (P)
– anti-HA
– anti-ß-Actin
Vector
HA-A0 Wt
HA-A0 S84A

Figure S3. MK2-mediated phosphorylation of hnRNPA0 in response to DNA damage induces binding to its target RNAs and cytoplasmic localization. Related to Figure 3. (A) Western blot analysis of whole cell lysates from cells expressing HA-tagged isoforms of hnRNPA0. A 2X HA tag induces slower migration on a SDS PAGE gel. Upper bands indicate exogenous hnRNPA0 and its phosphorylation upon DNA damage that is ablated by mutation of Serine 84 to Alanine.

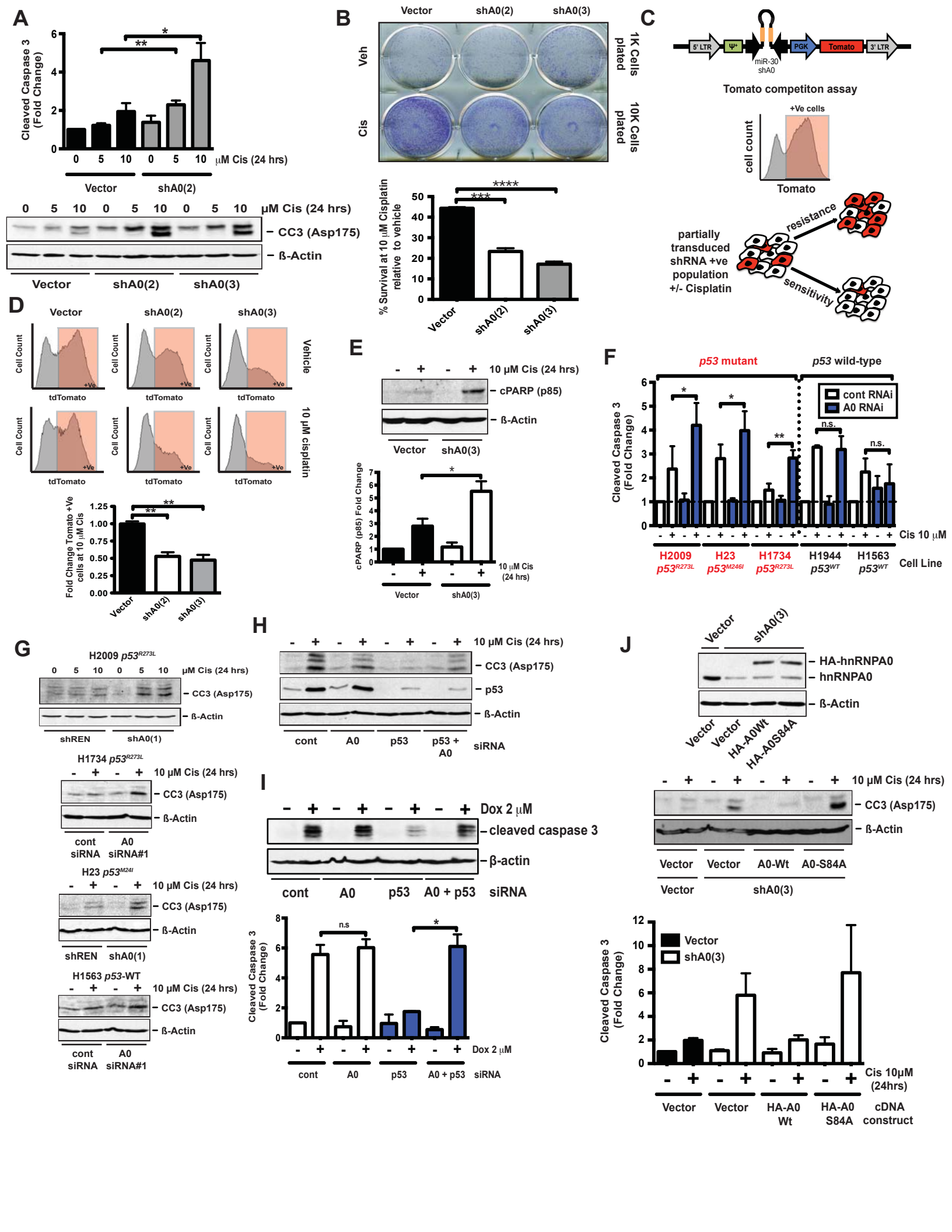
A
Cleaved Caspase 3 (Fold Change)
0 5 10 0 5 10 µM Cis (24 hrs)
Vector
shA0(2)
CC3 (Asp175)
ß-Actin
shA0(3)
B
Vector
shA0(2)
shA0(3)
Veh
Cis
1K Cells plated
10K Cells plated
% Survival at 10 µM Cisplatin relative to vehicle
C
5' LTR
Ψ+
miR-30 shA0
PGK
Tomato
3' LTR
Tomato competiton assay
+Ve cells
cell count
Tomato
partially transduced shRNA +ve population +/- Cisplatin
resistance
sensitivity
D
Vector
shA0(2)
shA0(3)
Cell Count
tdTomato
Vehicle
10 µM cisplatin
Fold Change Tomato +Ve cells at 10 µM Cis
E
10 µM Cis (24 hrs)
cPARP (p85)
ß-Actin
cPARP (p85) Fold Change
F
p53 mutant
p53 wild-type
cont RNAi
A0 RNAi
Cleaved Caspase 3 (Fold Change)
n.s.
Cis 10 µM
H2009 p53R273L
H23 p53M246I
H1734 p53R273L
H1944 p53WT
H1563 p53WT
Cell Line
G
H2009 p53R273L
CC3 (Asp175)
shREN
shA0(1)
H1734 p53R273L
cont siRNA
A0 siRNA#1
H23 p53M24I
H1563 p53-WT
H
CC3 (Asp175)
p53
cont
A0
p53
p53 + A0
siRNA
I
Dox 2 µM
cleaved caspase 3
ß-actin
cont
A0
p53
A0 + p53
siRNA
n.s
J
Vector
shA0(3)
HA-hnRNPA0
hnRNPA0
HA-A0Wt
HA-A0S84A
A0-Wt
A0-S84A
Vector
shA0(3)
Vector
shA0(3)
Cis 10µM (24hrs)
HA-A0 Wt
HA-A0 S84A
cDNA construct

Figure S4. Synthetic lethality between hnRNPA0-loss and a defective p53 pathway in response to chemotherapy. Related to Figure 4. (A) Depletion of hnRNPA0 with a second shRNA sensitizes murine lung adenocarcinoma cells to cisplatin. KP7B cells were transduced with a miR-30 retrovirus expressing a second hnRNPA0-specifc shRNA and treated as indicated. Error bars represent mean +/- SEM, n=3 experiments. * $p < 0.05$, ** $p < 0.01$,. **(B)** Long term survival of hnRNPA0-depleted cells is compromised upon cisplatin treatment. Colony formation assay of KP7B cells transduced with two independent hnRNPA0-targetting shRNAs. 10 fold more cells were plated in the vehicle conditions. Bars represent percent survival at 10 μM normalized first to vehicle treated cells for each condition then relative to vector only cells. Error bars represent mean +/- SEM, n=3 experiments. *** $p < 0.001$, **** $p < 0.0001$ **(C)** Fluorescence-based competition assays confirm that hnRNPA0 depletion confers a survival disadvantage in the face of cisplatin treatment. Schematic representation of the competition assay. Briefly KP7B cells were partially (~20-50%) transduced with empty vector carrying tdTomato or two different hnRNPA0 shRNAs also carrying tdTomato. Cells were treated with vehicle or 10 μM cisplatin for 48 hrs followed by extensive washing and incubation for 24 hrs in complete medium without drug. tdTomato positive cells was measured flow cytometry **(D)** if an shRNA confers no selective advantage or disadvantage to the cells that carry it the fold change between vehicle and drug treated cells should be 1, as seen for vector only cells, lower panel. However, if an shRNA confers sensitivity to a drug, shRNA-expressing cells will be selectively depleted from the mixed population resulting in a fold-change less than 1 as seen for both hnRNPA0 shRNAs. Error bars represent mean +/- SEM, n=3 experiments. ** $p < 0.01$. **(E)** Depletion of hnRNPA0 enhances cisplatin-induced PARP cleavage. Representative western blot for cleaved PARP (p85) from KP7B cells treated as in Figure 4. Bars represent mean +/- SEM n= 4 experiments, * $p < 0.05$. **(F)** Depletion of hnRNPA0 confers sensitivity to cisplatin in a panel of *p53*-mutant but not *p53*-WT lung adenocarcinoma cells. Measurements of cleaved caspase 3 in NSCLC cells depleted of hnRNPA0 either by A0 siRNA (H1734, H1563 and H1944) or shA01

(H2009 and H23). Data are expressed as fold change relative to control RNAi vehicle treated cells for each cell line. These data were used to generate fold changes represented in Figure 4D. Bars represent mean +/- SEM, n=3-5. * $p < 0.05$, ** $p < 0.01$. **(G)** Representative western blots of data depicted in Figure 4D and S4F. **(H)** Representative western blot for data shown in Figure 4G. **(I)** Acute p53 knockdown renders *p53*-WT A549 cells susceptible to hnRNPA0-loss induced chemo-sensitization. *p53*-WT A549 cells were transfected with the indicated siRNAs for 48 hrs followed by treatment with 2 μM doxorubicin for 24 hrs and measurement of cleaved caspase 3. Bars represent mean +/- SEM n=3. * $p = < 0.05$. **(J)** hnRNPA0-induced chemo-resistance requires the MK2 phosphorylation site. Upper panel, western blot for hnRNPA0 of KP7B with hnRNPA0 knockdown reconstituted with wild-type or S84A mutant human HA-tagged hnRNPA0 cDNAs. Note comparable levels of expression of exogenous HA-hnRNPA0 to that of endogenous hnRNPA0 in the absence of knockdown (compare first lane with third and fourth lanes). Middle panel, representative cleaved caspase 3 blot of KP7B cells treated with 10 μM cisplatin for 24 hrs. Lower panel, quantification of 4 independent experiments, bars represent mean +/- SEM.

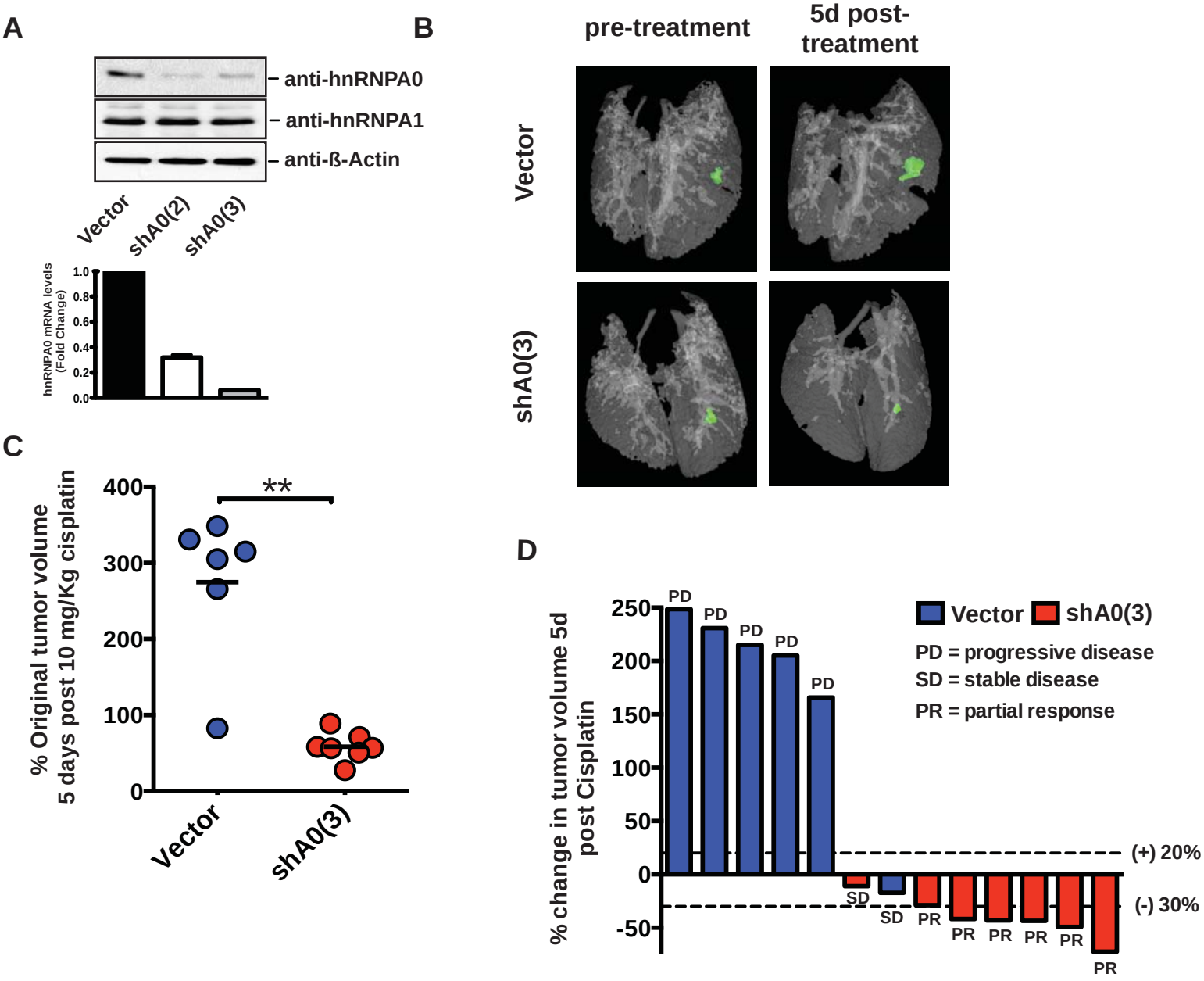
A
anti-hnRNPA0
anti-hnRNPA1
anti-ß-Actin
Vector
shA0(2)
shA0(3)
hnRNPA0 mRNA levels (Fold Change)
1.0
0.8
0.6
0.4
0.2
0.0
B
pre-treatment
5d post-treatment
Vector
shA0(3)
C
% Original tumor volume 5 days post 10 mg/Kg cisplatin
400
300
200
100
0
**
Vector
shA0(3)
D
% change in tumor volume 5d post Cisplatin
250
200
150
100
50
0
-50
PD
PD
PD
PD
PD
SD
SD
PR
PR
PR
PR
PR
(+) 20%
(-) 30%
Vector
shA0(3)
PD = progressive disease
SD = stable disease
PR = partial response

Figure S5. Decreased hnRNPA0 activity promotes cisplatin efficacy against *p53*-defective non-small cell lung cancer (NSCLC) *in vivo*. Related to Figure 5. (A) Validation of hnRNPA0 knockdown efficiency in KP7B cells by western blot and qRT-PCR (Bar chart). Note no difference in expression of the closely related hnRNPA1. **(B)** microCT imaging confirms enhanced tumor response of hnRNPA0-depleted tumors to cisplatin-based chemotherapy. 3D reconstruction of the same mouse lungs before treatment and 5 days after a single dose of 10 mg/Kg cisplatin, Green area highlights tumor mass. **(C)** hnRNPA0-depleted tumors regress in response to a high dose of cisplatin. Quantification of the largest tumor volume in each animal 5 days after treatment with a single dose of 10 mg/Kg cisplatin displayed as percent tumor volume relative to pre-treatment. Black line indicates the mean, each colored dot represents a single animal. ** $p < 0.01$. **(D)** Waterfall plot representation of percent change in tumor volume from the initiation of treatment to 5 days following cisplatin treatment. All bar one control animal (blue bars) had progressive disease (greater than a 20% increase in tumor volume) 5 days following chemotherapy whereas all bar one hnRNPA0-depleted tumor bearing animal (red bars) had a partial response (greater than 30% tumor shrinkage) by RECIST (Response Evaluation Criteria In Solid Tumors**)** criteria.

A

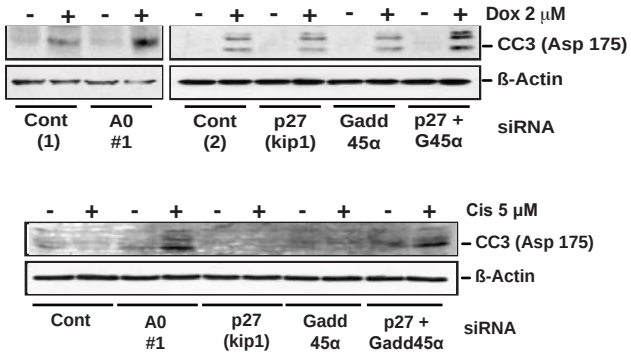

B

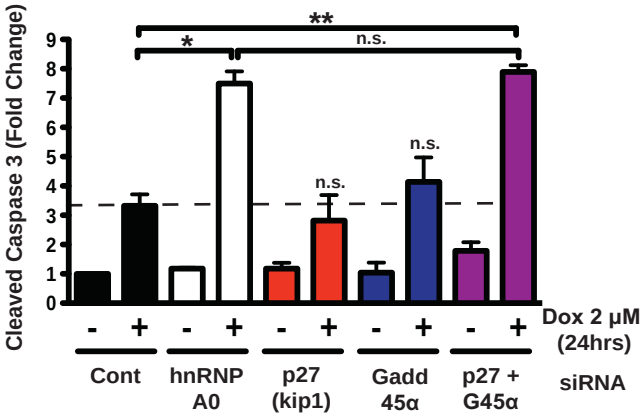

C

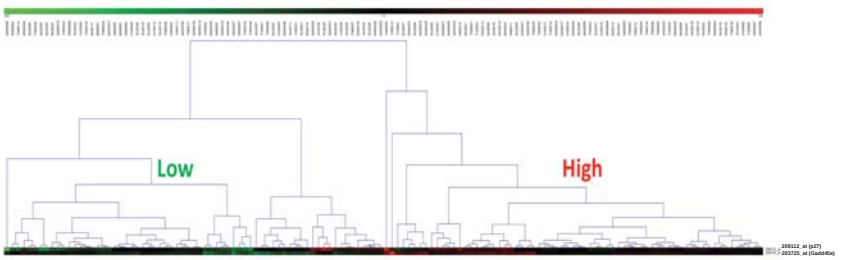

D

Gene	Expression	HR	95%CI	p value
p27	Low	0.56	0.22-1.44	0.229
	High	0.65	0.23-1.91	0.437
GADD45A	Low	0.42	0.17-1.07	0.068
	High	0.98	0.32-3.02	0.973
p27 and GADD45A	Low	0.26	0.07-0.94	0.04
	High	1.21	0.23-6.26	0.821

E

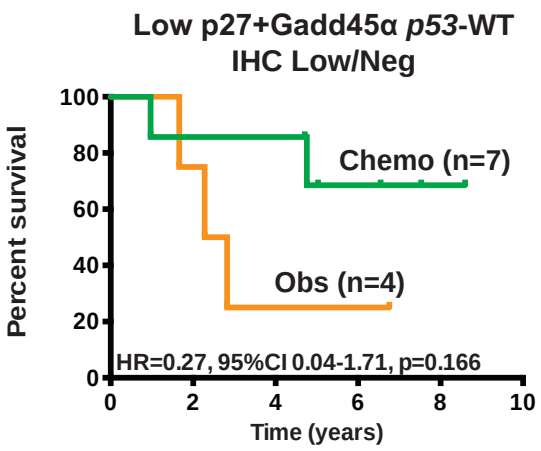

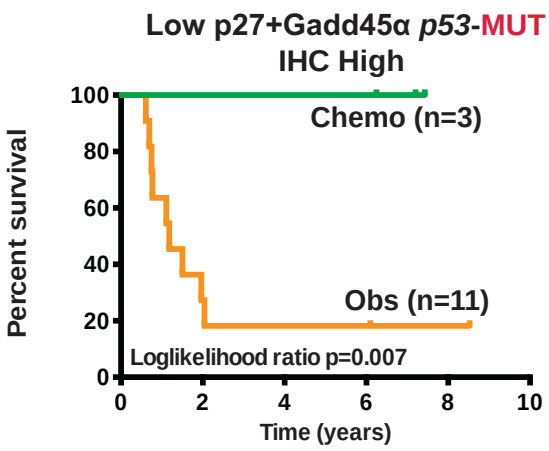

F

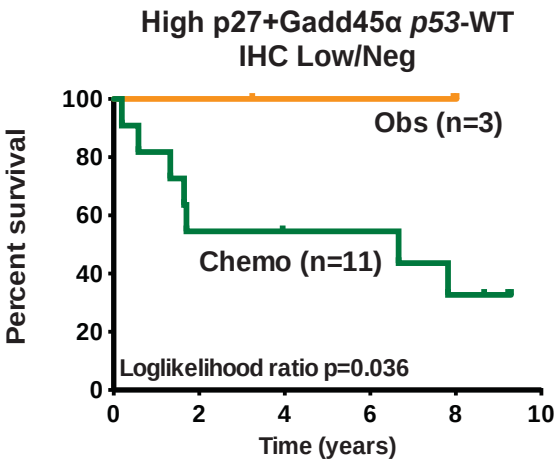

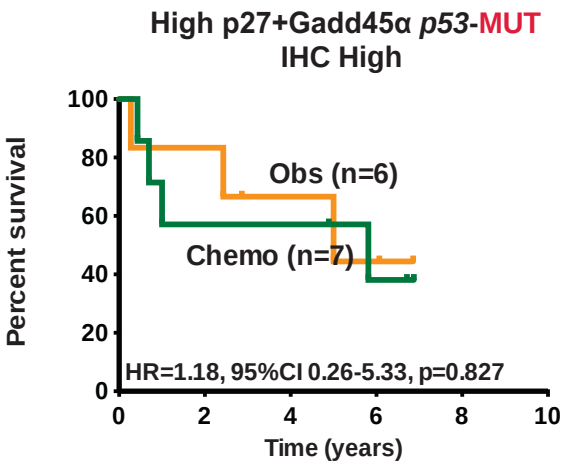

Figure S6. hnRNPA0 promotes resistance to chemotherapy through p27 and Gadd45α. Related to Figure 6. (A) Representative western blots of data quantified in Figure 6B and S6B. **(B)** Combined knockdown, but not single knockdown, of p27 and Gadd45α phenocopies the effect of hnRNPA0 loss on doxorubicin-induced cell death. H1299 cells were transfected with the indicated siRNAs and analyzed as in Fig 6A. Error bars represent mean +/- SEM, n=3 experiments. * $p < 0.05$, ** $p < 0.01$, n.s.=not significant. **(C)** Expression of $p27^{Kip1}$ and Gadd45α mRNAs in 133 non-small cell lung cancer samples profiled by using Affymetrix U133A (Zhu et al., 2010) represented by probe set 209112_at and 203725_at, respectively. Two clusters were identified based on the expressions of $p27^{Kip1}$ and Gadd45α using hierarchal clustering (Sturn et al., 2002). The 2 clusters were defined as low and high expressed groups based on the expression of these two genes. **(D)** Only the cluster that considers expression of both $p27^{kip1}$ and Gadd45α together, but neither alone, is significantly associated with therapeutic response in NSCLC patients. **(E-F)** Patients from (Fig 6C-D) were stratified into *p53*-WT and mutant groups by p53 IHC scores where possible: p53 IHC Low/Neg (wildtype) <15% tumor cells stain positively for p53 expression vs p53 IHC High (mutant) >15% tumor cells stain positively for p53 expression.

A

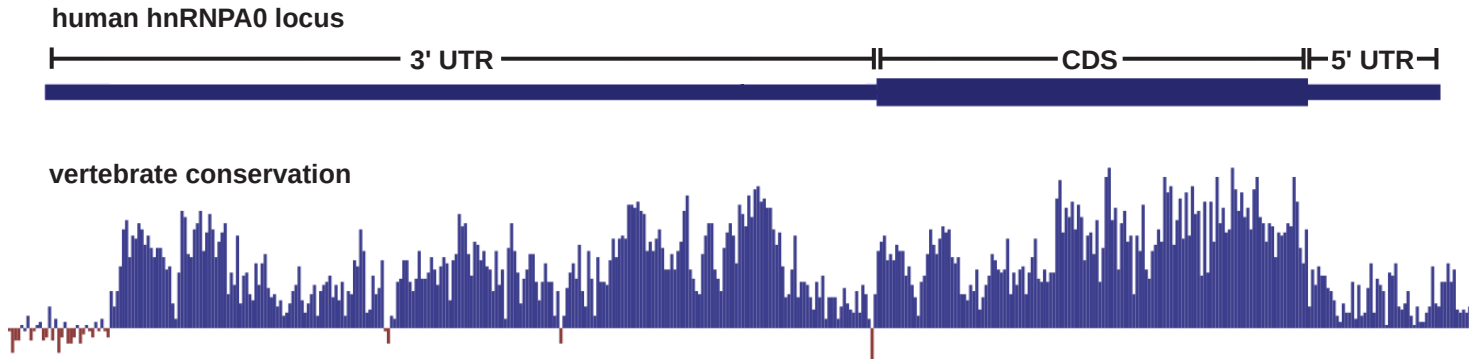
human hnRNPA0 locus
3' UTR
CDS
5' UTR
vertebrate conservation

B

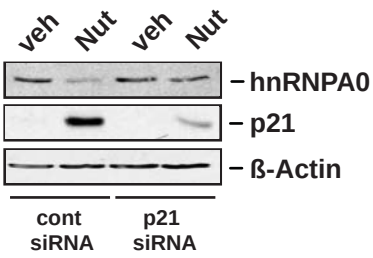
veh
Nut
veh
Nut
hnRNPA0
p21
ß-Actin
cont siRNA
p21 siRNA

Figure S7. Figure 7. The primary p53/p21 axis actively suppresses the sucessor hnRNPA0. Related to Figure 7.

(A) UCSC genome browser representation of the hnRNPA0 locus. Schematic depicts the vertebrate base-wise conservation below the hnRNPA0 gene architecture. The hnRNPA0 3′ UTR is highly conserved, more so than parts of the coding region, suggesting the existence of functional regulatory elements. **(B)** p21-dependent repression of hnRNPA0 upon p53 activation. A549 cells were transfected with a control siRNA or a p21-targeting siRNA for 48 hrs, followed by treatment with 10 μM Nutlin 3a for 24 hrs. p21 and hnRNPA0 protein expression were measured by western blot.

Supplementary Experimental Procedures

Retro-virus production

For VSVG-pseudotyped virus production, 293T cells were transfected using the calcium phosphate method (Clontech) using either pMLP (for shRNAs in H1299 cells), pMLS-tomato (for shRNAs in KP7B cells) or pLNCX2 (for HA-hnRNPA0 expression) along with packaging and structural vectors VSVG and GAG/POL. Supernatants containing virus were then used to transduce target cells in the presence of 8 ug/mL polybrene for three rounds of infection. Successfully transduced cells were selected either with puromycin (3 ug/mL) for pMLP infected cells, G418 for pLNCX2 infected cells (200 ug/mL) or were sorted for tdTomato expression by flow cytometry for pMLS-tomato infected cells. GFP-Luciferase was used to infect KP7B cells for bio-luminescent imaging and was a kind gift from Bonnie Huang (MIT).

Expression and purification of recombinant hnRNPA0 RNA recognition domains (RRMs).

The vector for expression of recombinant RRMs was derived from pET-28a (Novagen). It was modified to introduce a N-terminal His6-MBP tag and TEV cleavage site into the protein sequence (hnRNPA0 residues 1-181). The tagged protein was expressed in Rosetta 2 cells (Novagen) grown in TB and purified from cell lysate using a Ni-Sepharose column (GE Healthcare) and an amylose column (New England Biolabs). After TEV cleavage the sample was loaded back onto the Ni-Sepharose column. The RRMs stick to the column but come off in an imidazole gradient before the tag. The RRMs were further purified using a HiLoad 16/60 Superdex-75 column (GE Healthcare), dialyzed into a low salt buffer (10 mM TRIS pH8, 50 mM NaCl, 2 mM DTT), concentrated to 65 mg/ml by ultrafiltration (Millipore), flash frozen in LN_2 in 50 mL aliquots, and stored at -80 °C until needed.

Electromobility shifts assays (EMSAs) for *in vitro* RNA binding analysis.

A fragment of the p27 3′ UTR encompassing nucleotides 1821-1983 of the cdkn1b/p27 transcript was cloned from cDNA into pGEM-T (Promega). A fragment encompassing the first ~120 nucleotides of the Firefly Luciferase coding sequence was cloned into pGEM-T to serve as a negative control. Correct clones were linearized by Spe1 digest and used as templates for *in vitro* transcription with the T7 RiboMax kit (Promega) according to the manufacturers' protocol except that α-^{32}P UTP was used in place of UTP. After 4 hrs incubation at 37°C reactions were treated with RQ DNAse for 15 min and subject to acid phenol:chloroform extraction (Ambion). Probes were counted and 50,000 cpm of probe were used per reaction in EMSA binding buffer (40 mM Tris pH8, 30 mM KCl, 1mM $MgCL_2$, 0.01% NP40, 1 mM DTT) supplemented with 1 mg/mL BSA, 1 mg/mL yeast tRNA and increasing molar ratios of purified recombinant hnRNPA0 RRMs. Reactions were incubated at 30°C for 30 mins and then separated in 8% Acrylamide/TBE gels. Gels were dried down and exposed to phosphorimaging screens overnight. Quantification was performed using Quantity One (Bio-Rad) with signal migrating slower than free probe classified as bound and expressed as a percentage of unbound probe with background correction.

Immuno-flourescence microscopy.

H1299 cells were seeded onto glass coverslips in 12 well plates followed by treatment with doxorubicin for 16 hrs. Cells were fixed with 4% paraformaldehyde or 20 mins at room temperature, blocked in 10% goat serum and incubated with primary anti-HA antibody for ~2 hrs. Following primary antibody cells were washed in PBS and incubated with goat-anti-mouse-alexa-647 (Invitrogen/Life technologies/Molecular probes #A-21235) and Hoechst for 1 hr at room temperature. Coverslips were inverted onto glass slides and slides were imaged on a Zeiss Axioplan II upright microscope.

Cell Culture, antibodies and chemicals

All human cell lines were purchased from ATCC (American Type Culture Collection). H1299, H23, H1944, H1734 and H1563 cells were grown in RPMI supplemented with 10% FBS and L-Glutamine. 293T, A549, H2009 and KP7B cells were grown in DMEM supplemented with 10% FBS and L-Glutamine. KP7B cells were described previously (Doles et al., 2010). Antibodies against hnRNPA0 (#4046), hnRNPA1 (D21H11#8443), $p27^{Kip1}$ (D37H1#3688), MK2/MAPKAPK2 (#3042), cleaved PARP Asp 124 (mouse specific, 7C9 #9548) and Cleaved Caspase 3 D175 (5A1E#9664) were purchased from Cell Signaling Technologies. Phospho-Ser-84 hnRNPA0 antibody (#07-566) and lamin-A/C antibody (clone 14#05-714) were purchased from Upstate/Millipore. P53 (D01) antibody was purchased from Santa Cruz biotechnology. HA antibody (16B12) for immuno-flourescence was purchased from Covance and HA antibody (12CA5) for western blot was purchased from Roche. β-Actin antibody, γ-tubulin antibody, Actinomycin D, nocodazole, propidium iodide, doxorubicin, cisplatin and Nutlin 3a were purchased from Sigma Alldrich all chemicals were used at the indicated doses.

Survival Assays

For colony formation assays KP7B or SM1 cells were either vehicle treated or treated with cisplatin for 4 hr. Cells were then washed, trypsinized and re-plated at a concentration of 1000 cells for mock treated and 10,000 cells for cisplatin treated per well in a 6-well dish. After 10 days cells were fixed and stained with modified Wright-stain (Sigma-Aldrich). The imageJ ColonyArea plugin (Guzmán et al., 2014) was used to integrate signal from the whole well in an automated manner and surviving fractions were determined by normalization against vehicle treated cells. To measure the induction of cleaved caspase 3, cells were transfected or transduced as indicated with siRNAs or shRNAs then treated with cisplatin or doxorubicin as indicated for 24 hr harvested and analyzed by Western blot. For tomato competition assays, KP7B cells partially (20-50%) transduced with vector or hnRNPA0 targeting tomato-labeled shRNAs were treated with cisplatin for 48 hr followed by extensive washing, replenished media

and a further 24 hr recovery. Cells were then analyzed by flow cytometry to determine the percent tomato positive cells.

Flow Cytometry

For nocodozole trap cell cycle analysis H1299 cells were treated with doxorubicin at the indicated dose for 4 hr followed by addition of nocodazole at 100 ng/mL for an additional 24 hr. Cells were trypsinized and fixed in 70% ethanol in PBS for 24 hr. Following fixation, cells were resuspended in PBS containing 0.5% BSA and 10 ug/mL RNAse A for 30 min at 37^{o}C followed by the addition of 25 ug/mL propidium iodide. For EdU incorporation cells were pulse labeled for 1 hr with 10 μM EdU prior to cell harvest 16 hr after doxorubicin treatment as described previously (Cannell et al., 2010).

qRT-PCR primers

p27(kip1) hsa Fwd	gatgtcaaacgtgcgagtgt
p27(kip1) hsa Rev	ttgcaggtcgcttccttatt
Actin hsa Fwd	gaaaatctggcaccacacc
Actin hsa Rev	catactcctgcttgctgatcc
CDK2 hsa Fwd	gccctaatctcaccctctcc
CDK2 hsa Rev	aagggtggtggaggctaact
CycE hsa Fwd	agcggtaagaagcagagcag
CycE hsa Rev	tttgatgccatccacagaaa
CDK4 hsa Fwd	gaaactctgaagccgaccag
CDK4 hsa Rev	aggcagagattcgcttgtgt

CDK6 hsa Fwd	agagacaggagtggccttga
CDK6 hsa Rev	tgaaagcaagcaaacaggtg
CycD hsa Fwd	gaggaagaggaggaggagga
CycD hsa Rev	gagatggaaggggggaaagag
P19INK4D hsa Fwd	cccgtggggttatgtatcag
P19INK4D hsa Rev	tgtccaacacaccaaaagga
P18INK4C hsa Fwd	acgtcaatgcacaaaatgga
P18INK4C hsa Rev	tcagcttgaaactccagcaa
P16INK4A hsa Fwd	atatgccttcccccactacc
P16INK4A hsa Rev	cccctgagcttccctagttc
P15INK4B hsa Fwd	gaccgggaataaccttccat
P15INK4B hsa Rev	caccaggtccagtcaaggat
RB1 hsa Fwd	ggaagcaaccctcctaaacc
RB1 hsa Rev	tttctgcttttgcattcgtg
E2F1 hsa Fwd	atgttttcctgtgccctgag
E2F1 hsa Rev	atctgtggtgagggatgagg
hnRNPA0 hsa Fwd	gctttggcttcgtgacctac
hnRNPA0 hsa Rev	aactgcgagaagtgctcgat
p21 (Cip1) hsa Fwd	gacaccactggagggtgact
p21 (Cip1) hsa Rev	acaggtccacatggtcttcc
GAPDH hsa Fwd	gaaggtgaaggtcggagtcaac

GAPDH hsa Rev	cagagttaaaagcagccctggt
hnRNPA0 mmu Fwd	agtggtggatgtggctgttt
hnRNPA0 mmu Rev	ggtgctacatccgttggact
Actin mmu Fwd	tgttaccaactgggacgaca
Actin mmu Rev	ggggtgttgaaggtctcaaa

siRNA oligonucleotides and siRNA transfections

Silencer select siRNAs were purchased from Ambion: hnRNPA0 siRNA#1 (s21545 cat# 4392420), p27/cdkn1b siRNA (s2837 cat# 4390824), Gadd45a (s3992 cat# 4392420), p53 (s605 cat#4390624) negative control #1 (4390843). hnRNPA0 siRNA#2 was purchased from Dharmacon and used as a pool of two siRNAs (cat#J-012314-19-0005 and cat# J-012314-20-0005) a pool of two Dharmacon negative controls was used as a control (cat# D-001810-01-05 and cat# D-001810-02-05). For all combined knockdown experiments single knockdowns were equilibrated to equal RNA concentrations with appropriate control siRNA. siRNA transfections were performed using lipofectamine RNAiMax as per the manufacturer's instructions (Invitrogen) with a final concentration of 5 nM siRNA for silencer select siRNAs or 20 nM siRNA for Dharmacon siRNAs.

shRNA sequences

All shRNAs were designed using the cold spring harbor web portal (http://katahdin.cshl.org/siRNA/RNAi.cgi?type=shRNA) and 97mer oligonucleotides (see below for sequences, underlined sequences are gene-specific) were used as templates for PCR using miR-30 shRNA amplification primers (see below). Digested PCR products were ligated into either pMLP (puromycin resistant version of pMLS) or pMLS-Tomato.

shA0 mmu (1)

TGCTGTTGACAGTGAGCGCGCCCAGTTAGTGATGTTGAATTAGTGAAGCCA
CAGATGTAATTCAACATCACTAACTGGGCATGCCTACTGCCTCGGA

shA0 mmu (2)

TGCTGTTGACAGTGAGCGCACATGTACTGTGTAGTTTAAATAGTGAAGCCAC
AGATGTATTTAAACTACACAGTACATGTTTGCCTACTGCCTCGGA

shA0 mmu (3)

TGCTGTTGACAGTGAGCGCCCACATTTACTTGTAGCTGAGTAGTGAAGCCA
CAGATGTACTCAGCTACAAGTAAATGTGGATGCCTACTGCCTCGGA

shA0 mmu (4)

TGCTGTTGACAGTGAGCGATGCATCCATCTCTTTGTAATATAGTGAAGCCAC
AGATGTATATTACAAAGAGATGGATGCACTGCCTACTGCCTCGGA

shA0 hsa (1)

TGCTGTTGACAGTGAGCGAGCAGAGTAGCTGCGAAACAATTAGTGAAGCCA
CAGATGTAATTGTTTCGCAGCTACTCTGCCTGCCTACTGCCTCGGA

shA0 hsa (2)

TGCTGTTGACAGTGAGCGCAGACTTTACGTGTTAATTCTTTAGTGAAGCCAC
AGATGTAAAGAATTAACACGTAAAGTCTTTGCCTACTGCCTCGGA

shA0 hsa (3)

TGCTGTTGACAGTGAGCGCAGCCCTAAATTGCTATGACAATAGTGAAGCCA
CAGATGTATTGTCATAGCAATTTAGGGCTATGCCTACTGCCTCGGA

shMK2 hsa (1)

TGCTGTTGACAGTGAGCGATCCCTGGGTGTCATCATGTACTAGTGAAGCCA

CAGATGTAGTACATGATGACACCCAGGGACTGCCTACTGCCTCGGA

shMK2 hsa (2)
TGCTGTTGACAGTGAGCGAAGCGAAATTGTCTTTACTAAATAGTGAAGCCAC
AGATGTATTTAGTAAAGACAATTTCGCTCTGCCTACTGCCTCGGA

shMK2 hsa (3)
TGCTGTTGACAGTGAGCGAATCCAGTATCTGCATTCAATCTAGTGAAGCCAC
AGATGTAGATTGAATGCAGATACTGGATGTGCCTACTGCCTCGGA

shp27 hsa (1)
TGCTGTTGACAGTGAGCGATCTCTTAAAGTTGGAATTTACTAGTGAAGCCAC
AGATGTAGTAAATTCCAACTTTAAGAGAGTGCCTACTGCCTCGGA

shp27 hsa (2)
TGCTGTTGACAGTGAGCGATCAGAAGACGTCAAACGTAAATAGTGAAGCCA
CAGATGTATTTACGTTTGACGTCTTCTGAGTGCCTACTGCCTCGGA

shp27 hsa (3)
TGCTGTTGACAGTGAGCGCTCTGGTGATCTCCCAAGCTATTAGTGAAGCCA
CAGATGTAATAGCTTGGGAGATCACCAGATTGCCTACTGCCTCGGA

shGadd45a hsa (1)
TGCTGTTGACAGTGAGCGAGCTGAGTGAGTTCAACTACATTAGTGAAGCCA
CAGATGTAATGTAGTTGAACTCACTCAGCCTGCCTACTGCCTCGGA

shGadd45a hsa (2)
TGCTGTTGACAGTGAGCGACTGGAGGAAGTGCTCAGCAAATAGTGAAGCCA
CAGATGTATTTGCTGAGCACTTCCTCCAGGTGCCTACTGCCTCGGA

shGadd45a hsa (3)

TGCTGTTGACAGTGAGCGCGCAGTTACTCCCTACACTGATTAGTGAAGCCA
CAGATGTAATCAGTGTAGGGAGTAACTGCTTGCCTACTGCCTCGGA

shREN 702
TGCTGTTGACAGTGAGCGATACAAATTGTTAGGAATTATATAGTGAAGCCAC
AGATGTATATAATTCCTAACAATTTGTACTGCCTACTGCCTCGGA

miR-30 cloning XhoI Fwd
CAGAAGGCTCGAGAAGGTATATTGCTGTTGACAGTGAGCG

miR-30 cloning EcoRI Rev
CTAAAGTAGCCCCTTGAATTCCGAGGCAGTAGGCA

Supplementary References

Sturn, A., Quackenbush, J., and Trajanoski, Z. (2002). Genesis: cluster analysis of microarray data. Bioinformatics (Oxford, England) *18*, 207–208.

Wang, Y., Xiao, X., Zhang, J., Choudhury, R., Robertson, A., Li, K., Ma, M., Burge, C.B., and Wang, Z. (2013). A complex network of factors with overlapping affinities represses splicing through intronic elements. Nat. Struct. Mol. Biol. *20*, 36–45.

Zhu, C.Q., Ding, K., Strumpf, D., Weir, B.A., Meyerson, M., Pennell, N., Thomas, R.K., Naoki, K., Ladd-Acosta, C., Liu, N., et al. (2010). Prognostic and Predictive Gene Signature for Adjuvant Chemotherapy in Resected Non-Small-Cell Lung Cancer. Journal of Clinical Oncology *28*, 4417–4424.